

Stochastic EXIT Design for Low-Latency Short-Block LDPC Codes

Koike-Akino, Toshiaki; Millar, David S.; Kojima, Keisuke; Parsons, Kieran

TR2020-027 March 11, 2020

Abstract

We introduce a stochastic version of extrinsic information transfer (EXIT) chart which accounts for dispersion in finite-length LDPC decoding. The proposed approach can design short LDPC codes systematically, achieving about 1.2 dB gain over recently proposed scattered EXIT design.

Optical Fiber Communication Conference and Exposition and the National Fiber Optic Engineers Conference (OFC/NFOEC)

This work may not be copied or reproduced in whole or in part for any commercial purpose. Permission to copy in whole or in part without payment of fee is granted for nonprofit educational and research purposes provided that all such whole or partial copies include the following: a notice that such copying is by permission of Mitsubishi Electric Research Laboratories, Inc.; an acknowledgment of the authors and individual contributions to the work; and all applicable portions of the copyright notice. Copying, reproduction, or republishing for any other purpose shall require a license with payment of fee to Mitsubishi Electric Research Laboratories, Inc. All rights reserved.

Stochastic EXIT Design for Low-Latency Short-Block LDPC Codes

Toshiaki Koike-Akino, David S. Millar, Keisuke Kojima, Kieran Parsons

Mitsubishi Electric Research Laboratories (MERL), Cambridge, MA 02139, USA. koike@merl.com

Abstract: We introduce a stochastic version of extrinsic information transfer (EXIT) chart which accounts for dispersion in finite-length LDPC decoding. The proposed approach can design short LDPC codes systematically, achieving about 1.2 dB gain over recently proposed scattered EXIT design. © 2020 The Author(s)

OCIS codes: (060.4510) Optical comms., (060.1660) Coherent comms., (060.4080) Modulation.

1. Introduction

A great amount of efforts in developing high-gain forward error correction (FEC) codes has been put forward next-generation optical communications, e.g., low-density parity-check (LDPC) codes [1–5], staircase codes [6,7], turbo product codes (TPC) [8–10], and polar codes [11]. The design of short-length codes is of importance for ultra-low-latency communications [12]. However, LDPC codes cannot be readily designed with existing methods such as extrinsic information transfer (EXIT) chart which is based on the asymptotic (infinite length) behavior. For finite-length LDPC codes, the decoding trajectories are deviated from the analytical EXIT curves as observed in [15], where the convergence behavior was empirically analyzed using an “EXIT band chart”. In [16], the dispersion is theoretically analyzed to derive the lower-bound of block error rate (BLER), motivated by Polyanskiy’s normal approximation (NA). Recently, in [17], a scattered EXIT (S-EXIT) based on empirical decoding trajectory was introduced to design short LDPC codes. In this paper, we propose a new stochastic version of EXIT chart to design finite-length LDPC codes. The proposed method extends the iteration-aware EXIT trajectory design [5] for short LDPC code design, by introducing EXIT dispersion model. With the stochastic EXIT (St-EXIT), we can optimize LDPC codes under practical constraints of decoding latency and computational complexity by considering the number of edges in bipartite graph and decoder iterations. We demonstrate that St-EXIT offers 1.2 dB gain over S-EXIT design, approaching theoretical bounds.

2. Stochastic EXIT Design for Finite-Length LDPC Codes

Consider an irregular LDPC code having variable-node degree distribution $\lambda(x)$ and check-node degree distribution $\rho(x)$, where we use polynomial expressions; specifically, $\lambda(x) = \sum_d \lambda_d x^d$ and $\rho(x) = \sum_d \rho_d x^d$ denote degree distributions for LDPC codes having λ_d fraction of edges associated with degree- d variable nodes and ρ_d fraction of edges with degree- d check nodes. The extrinsic mutual information is asymptotically expressed as

$$I_{\text{vnd}} = \sum_d \lambda_d \cdot J \left(\sqrt{(d-1)(J^{-1}(I_{\text{cnd}}))^2 + (J^{-1}(I_{\text{ch}}))^2} \right), \quad I_{\text{cnd}} = 1 - \sum_d \rho_d \cdot J \left(\sqrt{d-1} \cdot J^{-1}(1 - I_{\text{vnd}}) \right), \quad (1)$$

where $J(\cdot)$ is the J-function [13]. At a code length of N bits, the generalized mutual information (GMI) between channel log-likelihood ratios (LLR) L_n and transmitted bits b_n is given as

$$I_{\text{ch}}(L; b) = 1 - \frac{1}{N} \sum_n \log_2(1 + \exp(-(-1)^{b_n} L_n)) \underset{N \rightarrow \infty}{=} 1 - \mathbb{E}_{L, b} [\log_2(1 + \exp(-(-1)^b L))]. \quad (2)$$

Note that the sample mean of channel GMI can approach the ensemble expectation if we have a large block length $N \rightarrow \infty$. However, for short-block LDPC codes, there are finite LLRs per codeword, and thus the empirical GMI can deviate from the nominal one. Fig. 1 shows the scattered EXIT chart [17] of variable-node decoder (VND) and check-node decoder (CND) across belief-propagation (BP) decoding of $N = 128$ (4,8)-regular LDPC codes. We can observe GMI dispersion from asymptotic EXIT curves due to the finite-sample mean.

In EXIT chart, L-value is modeled as a random variable following Gaussian distribution of $L_n \sim \mathcal{N}((-1)^{b_n} \sigma^2 / 2, \sigma^2)$ where $\sigma = J^{-1}(J)$. Therefore, finite-sample mean of GMI is also a random variable. Fig. 2 shows the channel GMI variance for $N = 1, 2, 4$, where we propose an accurate deviation model having a variance of $\delta_M = 2.68I(1-I)/M$ for a nominal GMI of I and the number of messages M . With the deviation model, we introduce a stochastic EXIT evolution where I_{ch} , I_{vnd} and I_{cnd} are propagated according to conventional EXIT in (1) with modification by a random perturbation via Gaussian noise having variances of δ_N , $\delta_{N\bar{d}}$, and $\delta_{N\bar{d}}$, respectively, where \bar{d} is the average variable-node degree. To track the nonlinear dynamics of extrinsic GMI distribution,

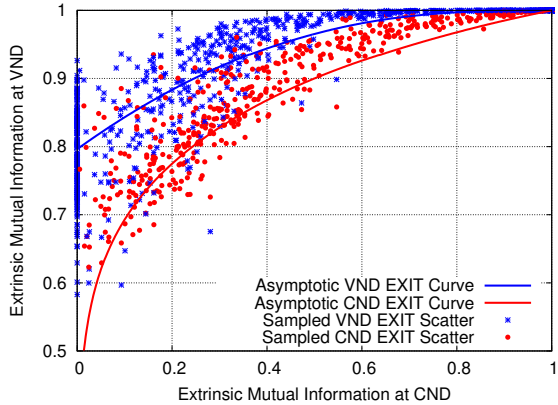


Fig. 1: S-EXIT [17] of $N = 128$ (4,8)-regular LDPC.

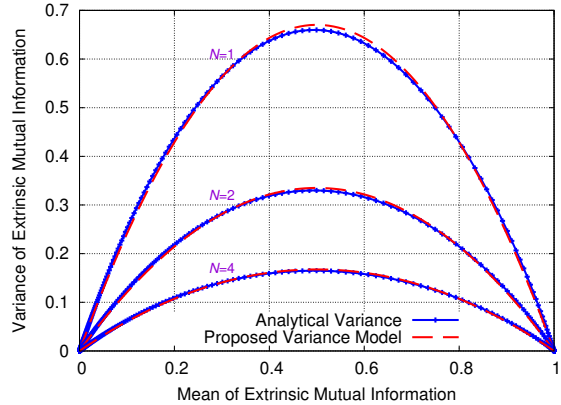


Fig. 2: Variance of extrinsic information.

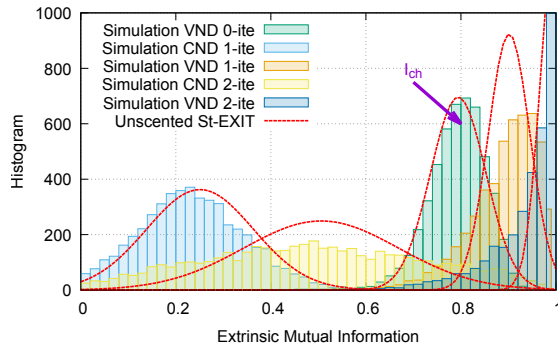


Fig. 3: Mutual information histogram over BP iterations of $N = 128$ (4,8)-regular LDPC (decoding simulation).

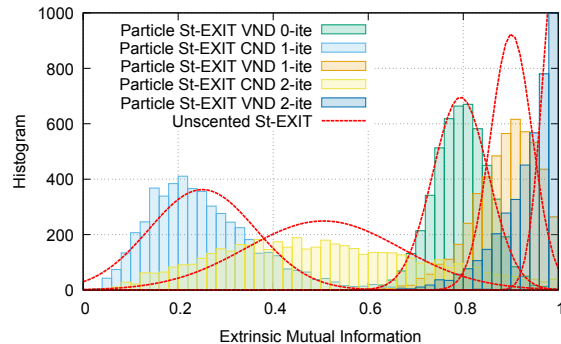


Fig. 4: Mutual information histogram over BP iterations of $N = 128$ (4,8)-regular LDPC (particle St-EXIT).

we can consider unscented transform or particle representation. Fig. 3 shows the extrinsic GMI histograms across simulated BP decoding. The unscented transform perfectly agrees with the distribution of initial decoding GMI I_{ch} with Gaussian variance of δ_{128} , whereas heavy tail distribution at later decoding iterations cannot be well-modeled by unscented transform. Fig. 4 shows the histogram of St-EXIT when using particle representation, i.e., Monte-Carlo sampling, which shows a good agreement of the simulated histogram in Fig. 3. Unlike S-EXIT design, St-EXIT does not need to simulate BP decoding but deviation model-based particle sampling. Given the number of iterations, St-EXIT searches for optimal degree distribution by sweeping values in $\lambda(x)$ and $\rho(x)$ such that expected bit-error rate (BER) of $\mathbb{E}[Q(J^{-1}(I_{app})/2)]$ is minimized, where I_{app} is the *a posteriori* GMI after particle sampling with $Q(\cdot)$ being the Q-function.

3. Design Comparison: St-EXIT vs. S-EXIT

We first verify that our St-EXIT can predict more accurate performance for finite-iteration short LDPC decoding. Fig. 5 shows the simulated BER performance of $N = 128$ regular LDPC code with 4-iteration flooding BP decoding. BER predictions via conventional EXIT and our St-EXIT are also present. Since the original EXIT assumes infinite-length codes, it exhibits a huge gap between simulation and estimated BER. Meanwhile, we can observe that the St-EXIT can provide remarkably accurate estimates of BER performance.

In Fig. 6, we then compare BLER performance of short LDPC codes, which are optimized by conventional EXIT trajectory, S-EXIT, and St-EXIT design methods. We use optimized degree distributions reported in [17], where EXIT and S-EXIT designs are used to optimize $N = 128$ half-rate LDPC codes as follows (node-perspective degree): $\lambda_{EXIT}(x) = 0.245x + 0.195x^2 + 0.07x^3 + 0.1x^4 + 0.39x^{14}$, $\lambda_{S-EXIT}(x) = 0.17x + 0.27x^2 + 0.08x^3 + 0.14x^4 + 0.04x^9 + 0.1x^{11} + 0.2x^{14}$. For St-EXIT, we imposed practical complexity constraint with limited average degree up to $\bar{d} = 3$, and obtained an optimized degree: $\lambda_{St-EXIT}(x) = 0.75x^2 + 0.18x^5 + 0.07x^8$. For each degree distribution, we evaluate BLER of 32-iteration layered decoding algorithm (LDA) for 100 LDPC codes ensemble, whose girth is maximized through the use of progressive edge growth (PEG) [18]. From Fig. 6, one can see that S-EXIT achieves a gain greater than 0.5 dB over the conventional EXIT design, that is consistent in [17]. Nevertheless, they did not account for finite-iteration decoding. Our St-EXIT offers further improvement of 1.2 dB gain over the S-EXIT, and approaches Gallager's random coding bound (RCB) and Polyanskiy's NA. More importantly, as we considered average degree in design for low-complexity applications, our LDPC code ($\bar{d} = 2.96$) is roughly two-fold faster decodable than the S-EXIT optimal code ($\bar{d} = 5.77$).

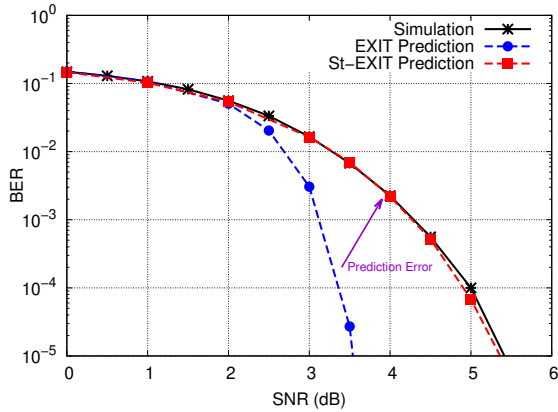


Fig. 5: BER prediction via EXIT or St-EXIT of $N = 128$ (4,8)-regular LDPC code (4-ite flooding BP).

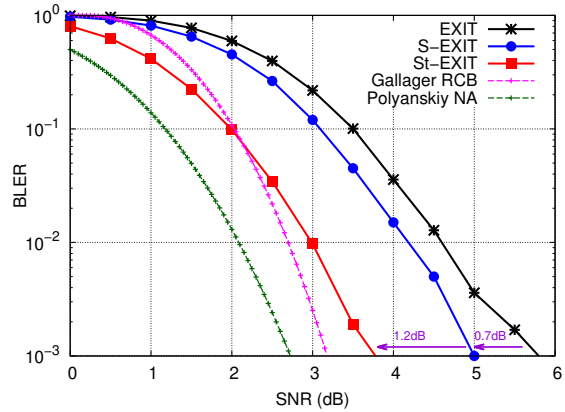


Fig. 6: BLER comparison between EXIT/S-EXIT/St-EXIT designs of $N = 128$ LDPC codes (32-ite LDA).

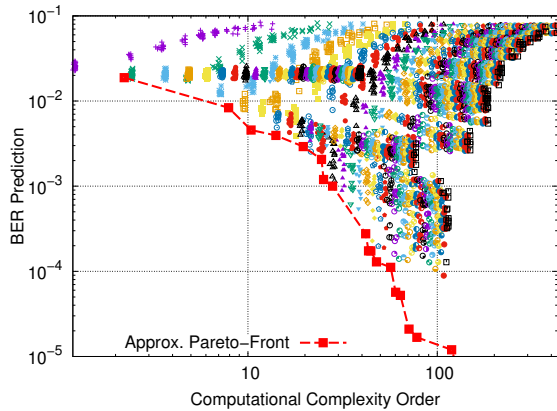


Fig. 7: Performance and complexity tradeoff with variable degree and decoding iterations (3 dB, $N = 128$).

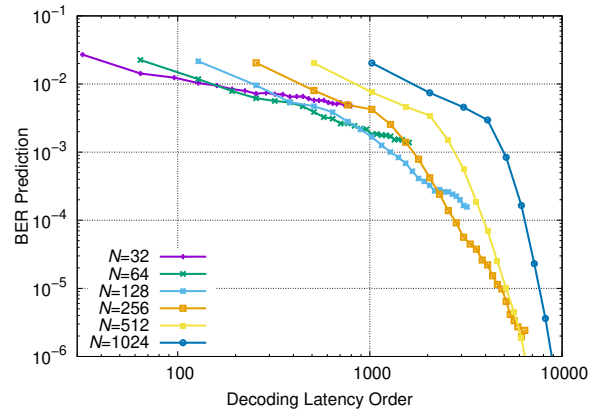


Fig. 8: Performance and latency tradeoff with variable length and decoding iterations ($N = 32, 64, \dots, 1024$).

In [5], we discussed Pareto optimization to jointly minimize BER and decoding complexity, which depends on average degree \bar{d} and decoding iterations N_{ite} . With St-EXIT, we can now consider also latency, which is a function of block length N and iterations N_{ite} . Fig. 7 shows the tradeoff between performance and complexity ($\mathcal{O}[\bar{d}N_{\text{ite}}]$), by varying degree distributions and decoder iterations. As mentioned in [5], more iterations with smaller average degree can outperform fewer iterations with larger average degree for some cases. Hence, we shall properly optimize the degree distribution to achieve Pareto-front between the complexity and performance criteria. Fig. 8 shows tradeoff between BER and latency ($\mathcal{O}[N N_{\text{ite}}]$) for the iteration-aware optimal degrees of different N and N_{ite} . It is found that more iterations with shorter codes can outperform fewer iterations with longer codes for some cases depending on the latency requirement and target BER. It suggests that degree design, iteration counts, and code length selection shall be jointly considered in Pareto sense to meet system requirement of performance, complexity and latency.

4. Conclusions

We proposed a new stochastic EXIT design for finite-length and finite-iteration LDPC decoding. The introduced particle representation of EXIT trajectory can track non-Gaussian dispersion evolution across decoder iterations, and hence our dispersion model can accurately predict BER performance of short LDPC codes. We verified that the proposed St-EXIT design offers higher performance up to 1.2 dB gain over recently introduced S-EXIT design at 128-bit short block length. It was also discussed that the St-EXIT can account for Pareto-optimal LDPC design to meet tradeoff among performance, complexity, and latency.

References

1. I. B. Djordjevic, *OFC* (2014): W3J-4.
2. L. Schmalen et al., *JLT* **33** 5 (2015): 1109–1116.
3. F. Buchali et al., *OFC* (2014).
4. A. Leven, L. Schmalen, *JLT* **32** 16 (2014): 2735–2750.
5. T. Koike-Akino et al., *JLT* **34** 2 (2016).
6. B. P. Smith et al., *JLT* **30** 1 (2012): 110–7.
7. C. Fougstedt, P. Larsson-Edefors, *OFC* (2018): Tu3C-6.
8. F. Paludi et al., *IEEE ISCAS* (2016): 429–32.
9. S. Dave et al., *OFC* (2011): JWA014.
10. T. Koike-Akino et al., *OFC* (2018): Tu3C.5.
11. T. Koike-Akino et al., *JLT* **36** 11 (2018), pp. 2248–58.
12. G. Liva, L. Gaudio, T. Ninacs, and T. Jerkovits, *CoRR* (2016).
13. S. ten Brink et al., *IEEE TCOM* **52** 4 (2004), pp. 670–8.
14. T.J. Richardson, M.A. Shokrollahi, R.L. Urbanke, *IEEE TIT* **47** 2, (2001)
15. J. W. Lee and R. E. Blahut, *IEEE TCOM* **55** 5 (2007), pp. 1033–43.
16. A. Abotabl and A. Nosratinia, *GLOBECOM* (2016).
17. M. Ebada, A. Elkelesh, S. Cammerer, and S. ten Brink, *ICC* (2018).
18. X.-Y. Hu et al., *IEEE TIT* **51** 1 (2005), pp. 386–98.